A comparison of MPAS and WRF meteorological models in California: 2013 winter and 2016 summer case studies

Kemal Gürer, Jeremy Avise and John Damassa

Air Quality Planning and Science Division, Air Resources Board, California Environmental Protection Agency, Sacramento, CA.

Abstract:

MPAS-A and WRF-ARW simulations were conducted for two 2-week periods during the Discover-AQ (January 10-24, 2013) and CABOTS (July 18-30, 2016) field campaigns in California's central valley. Output from both models were compared using horizontal and vertical cross sections of typical meteorological parameters, the temporal evolution of the meteorology at monitoring stations, 3D Lagrangian transport analysis, as well as statistical performance measures calculated over entire domain and at individual monitoring stations using the METSTAT and AMET modeling analysis packages.

Background:

The California Air Resources Board (CARB) is responsible for improving California's air quality, and photochemical modeling of regional air pollution forms the scientific basis for CARB's emissions control program. A major component of the regional air quality modeling efforts is the accurate representation of the regional meteorology that drives the majority of air pollution episodes within the state.

In CARB's current modeling system, WRF provides the meteorological inputs needed to drive the CMAQ (Appel et al., 2017) air quality modeling simulations. Given that MPAS looks to represent the future of meteorological modeling across multiple scales, it is advantageous to begin applying higher resolution MPAS over California to evaluate the ability of the model to simulate regional meteorology and compare those simulations to corresponding WRF simulations.

The numerical experiment:

The WRF model was setup using three two-way nested grids with 27, 9 and 3 km horizontal resolutions (Fig. 1a). The MPAS model was setup using a mesh with variable resolution from 3 to 48 km, where the 3 km resolution covers entire western USA and the resolution increases to 48 km outside of the region (Fig. 1b).

Both models were configured with 55 vertical layers, with first layer depth of 20 m and increasing to a maximum depth of 750 m above 6 km. The models were configured to use a consistent set of physics parameterizations, including NOAH LSM, Monin-Obukhov surface layer, YSU PBL, WSM 6-class and RRTM SW and LW radiation. One day of spin-up was added to the beginning of the model runs.
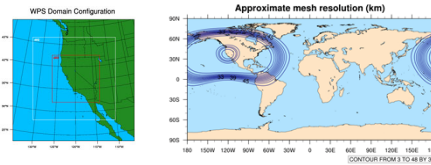

Figure 1: WRF nested 3-9-27 km grids (left) and MPAS 3-48m km variable mesh (right).

Results:

Figures 2a-c compare WRF and MPAS output for surface winds (a), temperature (b), and relative humidity (c) averaged over January 10-23, 2013 at 2:00 pm. Both models show similar wind, temperature, and relative humidity fields averaged over the two-week period. However, there are still some notable differences. For example, MPAS winds exhibit a more organized behavior over Pacific Ocean and its magnitude is slightly larger than that of WRF. MPAS temperature is cooler over NV, over higher elevations and over the southern San Joaquin Valley than that in WRF. MPAS relative humidity is slightly greater over NV, southern San Joaquin Valley and the Pacific Ocean, while slightly lower over southern California compared to WRF. Vertical cross section of vertical circulation and relative humidity (Fig 3) taken along west-to-east in the middle of the domain show that both models predict a similar vertical structure.
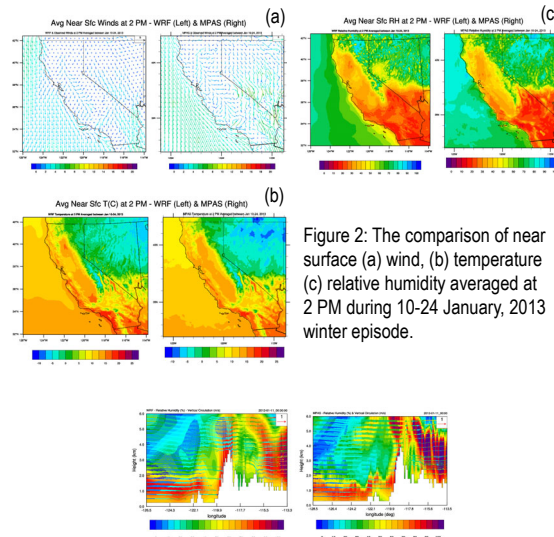

Figure 2: The comparison of near surface (a) wind, (b) temperature (c) relative humidity averaged at 2 PM during 10-24 January, 2013 winter episode.

Figure 3: The vertical cross section of circulation and relative humidity from WRF (left) and MPAS (right) at 00Z on Jan 11, 2013 along a line from west-to-east in the middle of the domain.

Comparison of the diurnal variation in near surface temperature (Fig 4a) shows that WRF tends towards a large bias at 16Z and drops to a small negative bias at night during the winter episode, while MPAS (Fig 4b) shows a steady near zero bias throughout the simulation over the same time period. Similarly, WRF exhibits a larger temperature bias at 14Z during the summer 2016 episode (Fig 4c), while MPAS shows a steady, ~0.5-0.7 C negative bias throughout the simulation (Fig 4d). The cause of this behavior is being investigated.
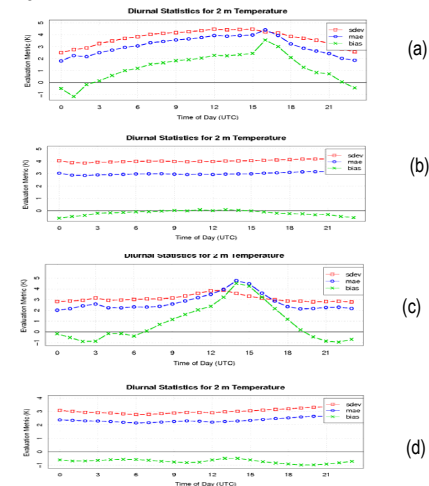

Figure 4: Diurnal variation in 2m temperature sdev, mae, and bias from a) WRF in winter 2013, b) MPAS in winter 2013, c) WRF in summer 2016, and d) MPAS in summer 2016.

Comparison of the time evolution of variables predicted by each model against observations at each station show that MPAS is superior at predicting near surface wind speed and temperature compared to WRF for both winter and summer episodes (Figs 5-8).
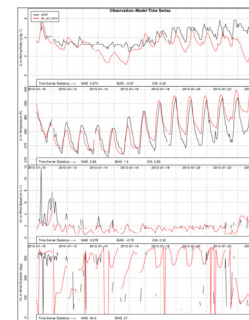

Figure 5: The comparison of WRF model variables against observations at Fresno, CA during 2013 winter episode.
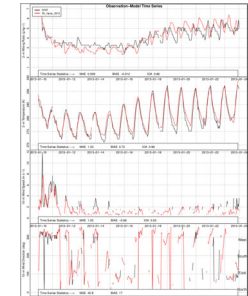

Figure 6: The comparison of MPAS model variables against observations at Fresno, CA during 2013 winter episode.
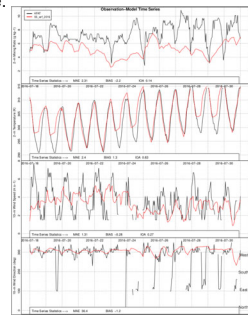

Figure 7: The comparison of WRF model variables against observations at Fresno, CA during 2016 summer episode.
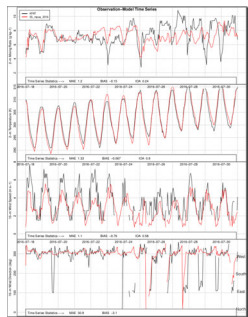

Figure 8: The comparison of MPAS model variables against observations at Fresno, CA during 2016 summer episode.

Disclaimer: